Cerebral Cortex January 2016;26:12–22
doi:10.1093/cercor/bhu165
Advance Access publication August 1, 2014

Functional Brain Activation Associated with Inhibitory Control Deficits in Older Adults

James P. Coxon[1,2,3], Daniel J. Goble[4], Inge Leunissen[3], Annouchka Van Impe[3], Nicole Wenderoth[3,5] and Stephan P. Swinnen[3,6]

[1]Movement Neuroscience Laboratory, Department of Sport and Exercise Science, [2]Centre for Brain Research, University of Auckland, Auckland, New Zealand, [3]Movement Control and Neuroplasticity Research Group, KU Leuven, Leuven, Belgium, [4]School of Exercise and Nutritional Sciences, San Diego State University, San Diego, CA, USA, [5]Neural Control of Movement Laboratory, Department of Health Sciences and Technology, ETH, Zurich, Switzerland and [6]Leuven Research Institute for Neuroscience & Disease (LIND), KU Leuven, Leuven, Belgium

Address correspondence to James P. Coxon, Movement Neuroscience Laboratory, Centre for Brain Research, University of Auckland, Auckland 1142, New Zealand. Email: j.coxon@auckland.ac.nz

In young adults, canceling an initiated action depends on the right inferior frontal cortex (IFC), presupplementary motor area (preSMA), and the basal ganglia. Older adults show response inhibition deficits, but how this relates to functional brain activation remains unclear. Using event-related functional magnetic resonance imaging, we tested whether older adults ($N = 20$) exhibit overactivation during stop-signal inhibition as shown for attentional control tasks, or reduced activity compared with young adults ($N = 20$). We used a modified stop-signal task involving coupled bimanual responses and manipulated whether both or just one hand was cued to stop. Stop-task difficulty was matched across groups. We found a group by condition interaction in supramarginal gyrus, anterior insula, rIFC, and preSMA, with activation increasing for successful Stop versus Go trials in the young adults only. Comparing the groups on Stop trials revealed preSMA and striatum hypoactivity for older adults. White matter tracts connecting rIFC, preSMA, and the subthalamic nuclei were associated with stronger activation of preSMA in older adults, suggesting that maintenance of the brain's structure has positive implications for brain function.

Keywords: aging, cognitive control, fMRI, response inhibition, stop signal

Introduction

A prominent theory of cognitive aging is that many behavioral changes stem from an inhibition deficit, impairing one's ability to filter out irrelevant information and suppress inappropriate responses (Hasher and Zacks 1988; Lustig et al. 2007; Healey et al. 2008). The construct of inhibition, broadly defined (Aron 2007), is likely subserved by at least 2 distinct neural mechanisms (Munakata et al. 2011): An indirect-competitive form where goal-relevant representations are facilitated and alternatives suppressed via diffuse lateral connectivity within cortical regions, and a directed-global form where processing is shutdown via connections with subcortical regions leading to cancelation of prepared movement. While it is conceivable that Stroop and Flanker decision tasks could be accomplished via the former mechanism, it is widely accepted that the latter direct type is recruited during stop-signal tasks, when time is of the essence (Aron 2007; Munakata et al. 2011).

There is convincing evidence to support an indirect-competitive inhibition deficit with older adults showing reduced suppression of distracting information during working memory tasks (Gazzaley et al. 2005; Clapp et al. 2011). Older adults also demonstrate performance decrements for attentional control tasks requiring indirect-competitive inhibition (e.g., Stroop and Flanker), with increased activation in the left prefrontal cortex often reported in addition to regions active in young adults (Nielson et al. 2002; Langenecker and Nielson 2003; Langenecker et al. 2004; Colcombe et al. 2005; Zysset et al. 2007). This has been interpreted as compensatory, similar to findings in the memory domain (Cabeza 2002; Cabeza et al. 2002), but for counterarguments see Nielson et al. (2002) and Colcombe et al. (2005). Accuracy was generally high in these studies, indicating that performance limits were not approached.

In contrast, much less is known about age-related neural alterations related to directed-global inhibition. Stop-signal tasks push each individual to their limit to determine stop-signal reaction time (SSRT), a measure of the latency of the process that underpins motoric inhibition. Older adults show stop-signal inhibition deficits (Kramer et al. 1994; Williams et al. 1999; Bedard et al. 2002) and white matter tracts between the right inferior frontal cortex (rIFC), presupplementary motor area (preSMA,) and subthalamic nucleus (STN) predict this decline (Coxon et al. 2012). However, functional magnetic resonance imaging (fMRI) studies investigating the directed-global form of inhibition in older adults are generally lacking (but see Sebastian et al. 2013 for a correlational lifespan approach).

In the current study, participants performed a modified stop-signal task probing the directed-global inhibition mechanism. Without providing the participant with any foreknowledge, either one or both components of a coupled bimanual response were cued for behavioral inhibition on Stop trials (Coxon et al. 2007). For the stop conditions in this task, inhibition is thought to occur by engaging a global inhibitory brake over all response components (Coxon et al. 2007, 2009, 2012; Macdonald et al. 2012; Aron et al. 2014; Bissett and Logan 2014). Both Stop one and Stop both conditions are infrequent and unexpected, and it has been argued that unexpected events engage global inhibition (Wessel and Aron 2013). Furthermore, the task allows for the measurement of action reprogramming. Both inhibition and action reprogramming deficits have been demonstrated in older adults (Coxon et al. 2012).

fMRI studies have shown that aging is associated with both increases and decreases of regional brain activity. Compared with young adults, older adults typically show increased brain activation when task difficulty is low, but reduced brain activation is often seen when task difficulty is high (Grady 2012). We have shown that older adults demonstrate reduced basal ganglia recruitment during complex motor task switching (Coxon et al. 2010). Here, we tested whether older adults exhibit evidence of overactivation during stop-signal inhibition, as previously reported for tasks probing indirect-competitive inhibition, or evidence of hypoactivity. We further hypothesized that stopping-related brain activity would be

associated with the microstructural organization of white matter connecting rIFC, preSMA, and STN in older adults (Coxon et al. 2012).

Method

Participants

Twenty elderly (mean age 68.7 years, range 62–81, 9 males) and 20 young adults (mean age 25.0 years, range 20–31, 9 males) with normal or corrected-to-normal vision participated in this fMRI experiment. All were right handed (laterality quotient: Old; mean 91.0, Young; mean 88.5). Participants scored within normal limits for the Mini-Mental State Examination (MMSE), indicating no clinical signs of dementia (Old, MMSE ≥27; Young MMSE ≥29; out of 30). The older participants were independent and community dwelling and had a similar number of years of formal education (Old; mean 16.6 years; Young; mean 18.1 years). The local ethics committee approved the procedure and all participants gave written informed consent.

Movement Prevention Task and Experimental Procedure

Participants performed a modified stop-signal task that probed both outright stopping and action reprogramming. Such measures are considered sensitive markers of predominantly top-down action control in the aging brain.

The default state on which stopping and action reprogramming were investigated was that of a spatially and temporally coupled bimanual response. For movements of this nature, the two hands are not programmed independently, but as a unified entity. Bimanual movements, especially those involving synchronous contraction of homologous muscles, are conceptually bound into a single action (Kelso et al. 1979; Wenderoth et al. 2009) and are associated with distinct bimanual signatures both within brain regions and across distributed brain networks (Tanji et al. 1988; Swinnen 2002; Swinnen and Wenderoth 2004). A cue to stop just one component of the bimanual response results in substantial response delays, and it is our assertion that these delays reflect inhibition of the bimanual action and action reprogamming to produce a unimanual response (Coxon et al. 2007, 2009, 2012; Macdonald et al. 2012).

Custom software generated a visual display that was viewed via a mirror attached to the head coil. Two vertical indicators moved from the bottom upwards, at an equal and constant rate, crossing a horizontal target line 800 ms from onset (Fig. 1). Participants received a standardized description during which task conditions were sequentially introduced. They were instructed to depress the mouse button switches, to look at the target line throughout the experiment, and to interrupt both indicators at this target by extending their left and right index fingers to release the switches (Go trials). It was emphasized that Go trials should be performed as accurately and consistently as possible. Next, it was explained that the indicator(s) would sometimes stop automatically before reaching the target and that when this happened, they should try to inhibit movement of the corresponding hand such that the switch was not released (Stop trials). Three possibilities were introduced: (1) Stop All (SA), in which both indicators stopped simultaneously prior to the target; (2) Stop Left (SL-GR), in which the left indicator stopped prior to the target; and (3) Stop Right (SR-GL), in which the right indicator stopped prior to the target. The latter conditions require action reprogramming, with SL and SR referring to the hand that was cued to stop, and GR and GL referring to the hand for which a new unimanual response was required (i.e., Go). Stopping could be made more or less difficult by altering the time that the indicator stopped prior to the target (Coxon et al. 2006, 2007). Participants were instructed that the experiment was designed to determine how much time they needed to inhibit movement. A short demonstration by the experimenter followed this description.

A Go trial consisted of a black warning rectangle for 500 ms, after which both indicators started to fill upward (Fig. 1*A*). When the subject simultaneously extended both fingers, the software recorded the response time relative to the target (in ms) for each response switch. One second after trial onset, the indicators were reset to empty. Stop trials were identical to Go trials up until the point at which either one, or both indicators stopped automatically before the target (Fig. 1*B–D*). When only one indicator stopped, the other indicator continued until the subject reprogrammed a unimanual response (e.g., SL-GR requires the subject to Go with the right hand).

Prescan Session

A behavioral experiment was performed in a dummy scanner to familiarize participants with the task and, critically, to determine individualized parameters for the scan session. First, participants practiced the task, performing Go trials + SA, then Go trials + SL-GR, and SR-GL, then all possible conditions combined (~10 min). They then performed a block consisting only of Go trials (40 trials) followed by 5 blocks of 100 trials containing Go (70%), SA (10%), SL-GR (10%), and SR-GL (10%) trials, presented in a random order. For the Stop conditions, there were 5 stop times, 10 trials per stop time, also randomized. For SA, both indicators stopped automatically 270, 230, 190, 150, and 110 ms prior to the target. Because ~30 ms more time is required on SL-GR and SR-GL trials (Coxon et al. 2007), for these conditions the indicator stopped automatically 300, 260, 220, 180, and 140 ms prior to the target.

The probability of responding, *P*(respond), was determined at each stop time, with *P*(respond) = 0 indicating consistently successful inhibition and *P*(respond) = 1 indicating that movement prevention was impossible. For each individual, the critical Stop Time (ST_{crit}) where *P*(respond) = 0.5 was determined [for details see Coxon et al. (2012)] and used to individually set the difficulty of the fMRI experiment.

Scanner Experiment

Within 1 week of the prescan session, participants performed the same task during fMRI. Each individual's prescan ST_{crit} values for each condition (SA, SL-GR, and SR-GL) were used to determine the stop times. This meant that older adults were given, on average, slightly more time to inhibit, accounting for their slower processing speed. Importantly, the stop task was challenging to perform and difficulty was matched across groups. There were 7 runs of 60 trials, each consisting of Go (70%), SA (10%), SL-GR (10%), and SR-GL (10%). The trials were presented in a pseudo-random order, interspersed with variable null time (33% of total scan time), and optimized for the contrast Stop > Go (using optseq2). The minimum time between trials was 3 s. In total, there were 420 trials: 294 Go trials, and 42 per stop condition. Each stop condition was parametrically modulated by stop time (3 levels, ST_{crit} + 60 ms, ST_{crit} + 30 ms, ST_{crit}).

Analysis of Behavior

Performance on Go trials was characterized by average Go trial response time, and its associated variability (1 SD of the response distribution). The stopping interference effect was quantified for the non-stopping hand (left hand for SR-GL and right hand for SL-GR) as the response time delay on successful Stop trials relative to Go trials, reflecting a global inhibitory brake mechanism and subsequent action reprogramming (Coxon et al. 2007). For the prescan session, SSRT was calculated by determining the difference between the ST_{crit} and mean Go trial response time. Calculating SSRT this way has been verified to give essentially identical results compared with the integration method (Coxon et al. 2012) due to a normal distribution of Go trial response times for this timed response paradigm. SSRT provides an index of stopping ability, such that individuals with faster SSRT's can be considered more adept at stopping.

For Go response time, Go response variability, and stopping interference effects, mixed analyses of variance (ANOVAs) with factors Group (Old and Young) and Session (pre and scan) were performed. The interaction effect was of primary interest; the null hypothesis being that the 2 groups did not differ as a function of testing session. As the most difficult stop time was set to equal ST_{crit} from the prescan session, we confirmed that *P*(respond) at ST_{crit} (A) did not differ across groups for the scan session (two-tailed independent samples *t*-test), and (B) did not differ from *P*(respond) = 0.5 (one-sample *t*-test for each group). SSRT was analyzed using ANOVA with factors Group and

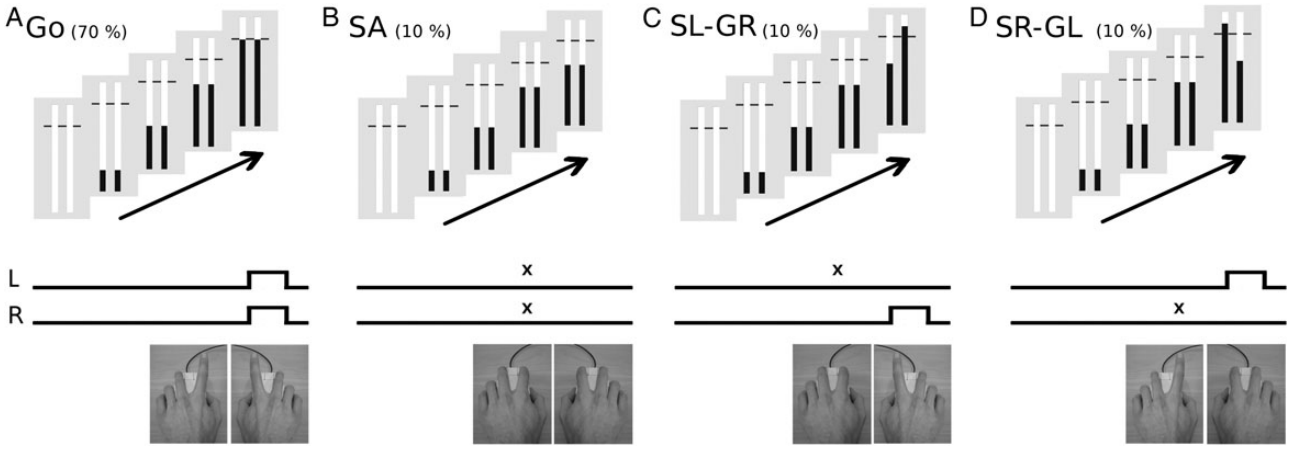

Figure 1. On every trial, participants prepared to simultaneously extend their left (L) and right (R) index fingers such that 2 continuously moving indicators were interrupted at a target, 800 ms from onset. (*A*) Go—on most trials, participants were required to respond as accurately as possible. (*B*) SA—when both indicators stopped automatically (*x*), the successful response was to prevent any movement. (*C* and *D*) SL-GR and SR-GL—when only one indicator stopped automatically, the successful response was to prevent movement of the corresponding hand, while still responding with the other at the target.

Condition (SA, SL-GR, and SR-GL) and subsequently interrogated with one-tailed *t*-tests due to the a priori hypothesis of prolonged SSRT in older adults (Kramer et al. 1994). For all *t*-tests, a modified Bonferroni correction was applied.

To confirm the parametric manipulation of stop-task difficulty in the scanner, a mixed ANOVA with factors Group (Old and Young) and Stop Time (ST_{crit} + 60 ms, ST_{crit} + 30 ms, and ST_{crit}) was performed for *P*(respond). For figures and tables, results are reported as mean ± standard error.

Image Acquisition and Preprocessing

A Siemens 3-T Magnetom Trio MRI scanner (Siemens, Erlangen, Germany) with a 12-channel head coil was used for image acquisition. For all subjects, structural imaging included: (1) A T_1-weighted magnetization-prepared rapid gradient-echo image [time repetition (TR) = 2300 ms, echo time (TE) =2.98 ms, 1 × 1 × 1.1 mm voxels, field of view: 240 × 256, 160 sagittal slices], (2) a T_2*-weighted fast low-angle shot image (TR = 30 ms, TE = 20 ms, flip angle =12°, matrix 192 × 256, 104 axial slices, 0.9 × 0.9 × 1.2 mm voxels), and (3) a diffusion-weighted single-shot spin-echo echoplanar image for diffusion tensor imaging (TR = 7200 ms, TE = 81 ms, flip angle = 90°, matrix 96 × 96, 56 sagittal slices, 2.19 × 2.19 × 2.2 mm voxels, 64 non-collinear directions, *b*-value 1000 s/mm^2). Functional data (fMRI) were acquired with a descending gradient echo planar imaging (EPI) pulse sequence for T_2*-weighted images (TR = 3000 ms, TE = 30 ms, flip angle = 90°, 50 oblique axial slices each 2.8 mm thick, interslice gap 0.028 mm, in-plane resolution 2.5 × 2.5 mm, 80 × 80 matrix). Three "dummy" scans at the beginning of each run were discarded from the fMRI analysis.

Image preprocessing was conducted using SPM5 (Wellcome Department of Imaging Neuroscience, University College, London, UK) within MATLAB 7.4 (Mathworks, Sherborn, MA, USA). EPI volumes were spatially re-aligned to the first volume in the time series, and then corrected for differences in slice acquisition time by temporal interpolation to the middle slice (reference slice = 25). The mean EPI image was normalized to the MNI functional template (EPI.nii) and the same transformation was applied to all EPI images. These normalized images (2.5 × 2.5 × 2.5 mm voxels) were spatially smoothed with an isotropic Gaussian kernel of 10 mm full-width at half-maximum.

Event-Related Hemodynamic Response Analysis

For subject-level analysis, events were specified at the time of indicator onset and modeled as delta functions convolved with the canonical hemodynamic response function (HRF) and its temporal derivative within a general linear model. Five conditions were specified: Go trials, successful SA trials, successful SL-GT trials, successful SR-GL trials, and unsuccessful Stop trials. Go trials were parametrically modulated by the recorded response times. Stop trials (SA, SL-GR, and SR-GL) were parametrically modulated as a function of the 3 stop times (ST_{crit} + 60 ms, ST_{crit} + 30 ms, and ST_{crit}). Realignment parameters were included as covariates of no interest to correct for head movement. Data were filtered in the temporal domain using a high-pass cut-off frequency of 1/128 Hz, and global differences in blood-oxygen level-dependent signal were removed by scaling to the grand session mean. For each subject, the contrasts Go, SA, SL-GR, and SR-GL were created by weighting the canonical HRF for each condition.

For every participant, translational head movement was <2 mm in each of the 7 runs. Correlations between the motion parameters and the experimentally derived conditions of interest (Go, SA, GL-SR, and SR-SL) in the design matrix were minimal for all participants and similar across groups (unsigned correlation coefficient *r*: Young group: grand mean 0.046, range 0.004–0.160; Old group: grand mean 0.045, range 0.004–0.157).

The first-level contrast images were used as input for random-effects (RFX) ANOVA with Group (Old and Young) and Condition (Go, SA, SL-GR, and SR-GL) as factors with unequal variance assumed. The contrast StopInhibit > Go (i.e., successful inhibition trials from all Stop conditions) was specified for each group separately. To examine group differences at the whole-brain level, we calculated the interaction (StopInhibit > Go_{Young}) > (StopInhibit > Go_{Old}), and vice versa. The groups were also compared for Go and StopInhibit trials separately. Additionally, a conjunction analysis (Nichols et al. 2005) was specified for each group to determine whether there were regions more active for Stop one (SL-GR and SR-GL) conditions than both SA and Go (SL-GR > SA ∩ SL-GR > Go ∩ SR-GL > SA ∩ SR-GL > Go). A height threshold of $P < 0.001$, $t > 3.14$, was used for all analyses and unless explicitly stated correction for multiple comparisons was at the cluster level using Gaussian random field theory and family-wise error (FWE) correction, $P < 0.05$.

Regions of Interest

We performed a region of interest analysis testing for the group by condition interaction within the right inferior frontal cortex (rIFC), the anterior portion of supplementary motor area (preSMA), globus pallidus (GP), and the STN. The IFC was determined by the union of Brodmann's areas 44 and 45, that is, pars opercularis and pars triangularis, from the Jülich Histological Atlas (>50% probability). The left and right GP and preSMA ($y > 0$) were taken from the automated anatomic labeling template. For STN, group MNI space masks were used based on manual delineation (Coxon et al. 2012). A height threshold of $P < 0.001$ was first applied to the whole-brain image and clusters were deemed

significant if $P < 0.05$, FWE corrected, after small volume correction within the anatomically defined ROIs.

White Matter Microstructural Organization Regression Analysis

Diffusion-weighted images were analyzed using FSL (Analysis group, FMRIB, Oxford University, Oxford, UK). The diffusion tensor model was fit to the data using the diffusion toolbox, from which fractional anisotropy (FA) was calculated. All subjects' FA images were registered to a common space (the FA158 MNI space template) using a combination of affine and non-linear registration. A mean FA image was created, eroded to an FA skeleton, and thresholded at FA >0.25. Probabilistic tractography (Behrens et al. 2007) was performed between the right IFC, bilateral preSMA, and bilateral STN ROIs outlined above (for more details see Coxon et al. 2012). The MNI space tract maps were thresholded at 0.02%, binarized, and summed across participants. Voxels that were present in > 95% of participants were retained. A combined right IFC–preSMA–STN tract mask was generated and the mean FA of all skeleton voxels within the mask was calculated for each participant. The resulting FA values were used in a regression analysis to predict StopInhibit > Go activation (whole brain, $P < 0.001$ uncorrected). This enabled us to test for a positive association between stopping activation and white matter microstructural organization in older adults.

Results

Behavior

The behavioral results from the prescan and scan sessions are summarized in Table 1. As expected, older adults' performance was slightly worse than the young group, with SSRT being significantly prolonged ($F_{1,38} = 14.8$, $P < 0.001$). Averaged across conditions, SSRT was 212 ms in the young group and 244 ms for the older adults. Importantly, Go performance remained stable across sessions, indicating that each individual's prescan session ST_{crit} was a valid approximation of ST_{crit} during the scan session. The probability of responding did not differ across groups for any of the stop conditions, indicating that stop-task difficulty was successfully matched during scanning. One-sample *t*-tests for *P*(respond) at ST_{crit} during the scan session found no significant deviation from *P*(respond) = 0.5. Finally, parametric modulation of stop-task difficulty in the scanner was confirmed by a significant main effect of Stop Time ($F_{2,76} = 184.8$, $P < 0.001$; Fig. 2). The Group × Stop Time interaction ($F_{2,76} = 5.0$, $P = 0.01$) was also significant.

Functional Magnetic Resonance Imaging

In the following sections, we investigate age-related differences in stopping, going, and action reprogramming. We also ask whether the microstructural organization of task-specific white matter tracts is associated with the ability to modulate brain activity for successful stopping in older adults.

Activation Associated with Stop-Task Difficulty in Each Group

The experimental design was optimized to detect activation for the contrast StopInhibit > Go. Previous work in young adults has revealed activity in bilateral anterior insula, right IFC, preSMA, and the basal ganglia (striatum and subthalamic nucleus) for this contrast (Aron and Poldrack 2006; Zandbelt and Vink 2010). Therefore, as a first step, we examined this contrast in each group separately and performed a conjunction analysis, to identify which brain areas were specifically activated by only the young or only the elderly, or commonly by both. Secondly, we tested for a group by condition (StopInhibit > Go) interaction at the whole-brain level, and within anatomically defined regions of interest to identify regions for which activity differs significantly between groups. Thirdly, we determined whether activity modulated as a function of action reprogramming requirements on Stop trials (Stop one vs. Stop both).

StopInhibit > Go

As expected, activation was observed in regions previously associated with successful stopping in young adults (Fig. 3*A*). Local maxima for right IFC pars opercularis, anterior insula, preSMA, and anterior cingulate cortex (Table 2) were all in excellent agreement (within 8-mm Euclidean distance) with the coordinates reported by Aron and Poldrack (2006). Activation was also evident in the left anterior insula, supramarginal gyrus, and bilateral basal ganglia extending into a region consistent with the structurally delineated STN (shown in green, Fig. 3*A*). The same StopInhibit > Go analysis for the older adults revealed only 2 clusters, both of which were in the parietal lobe and overlapped with active areas in the young group (Fig. 3*A* and Table 2).

Group by Condition Interaction

Having determined that older adults do not show the activation pattern typically observed in Young adults, we next tested whether the group by condition interaction (StopInhibit > Go_{Young}) > (StopInhibit > Go_{Old}) was significant at the whole-brain level. Clusters in anterior insula and supramarginal gyrus bilaterally survived correction for multiple comparisons (Fig. 3*B*), with a significantly greater increase in activation on StopInhibit trials for the young compared with the old group (Fig. 3*C*). We also tested for an interaction within each region

Table 1

Behavioral data for the prescan and scan sessions

	Prescan session		Scan session		Statistics		
	Old	Young	Old	Young	Group	Session	Interaction
Go time relative to target (ms)	27 ± 3.4	17 ± 2.3	26 ± 4.1	16 ± 2.4	$F_{1,38} = 5.9$, $P =$ **0.02**	$F_{1,38} = 0.2$, $P = 0.64$	$F_{1,38} = 0.01$, $P = 0.91$
Go variability (ms)	50 ± 2.0	34 ± 1.5	43 ± 1.6	30 ± 1.3	$F_{1,38} = 41.2$, $P <$ **0.001**	$F_{1,38} = 50.9$, $P <$ **0.001**	$F_{1,38} = 2.5$, $P = 0.12$
Interference effect SR-GL (ms)	142 ± 6.5	98 ± 9.0	120 ± 8.8	98 ± 7.3	$F_{1,38} = 10.6$, $P =$ **0.002**	$F_{1,38} = 5.2$, $P =$ **0.03**	$F_{1,38} = 5.4$, $P =$ **0.03**
Interference effect SL-GR (ms)	123 ± 7.5	81 ± 8.7	120 ± 7.0	81 ± 5.9	$F_{1,38} = 17.8$, $P <$ **0.001**	$F_{1,38} = 0.1$, $P = 0.71$	$F_{1,38} = 0.2$, $P = 0.68$
SA: SSRT (ms)	204 ± 4.7	189 ± 2.5			$P =$ **0.004**		
SL-GR: SSRT (ms)	245 ± 9.7	221 ± 4.5			$P =$ **0.018**		
SR-GL: SSRT (ms)	284 ± 13.9	226 ± 4.0			$P <$ **0.001**		
SA: ST_{crit} *P*(respond)			0.54 ± 0.05	0.60 ± 0.05	$P = 0.35$		
SL-GR: ST_{crit} *P*(respond)			0.46 ± 0.04	0.41 ± 0.05	$P = 0.45$		
SR-GL: ST_{crit} *P*(respond)			0.42 ± 0.05	0.41 ± 0.04	$P = 0.83$		

Note: For Go response time and interference effects, the Group × Session ANOVA is reported. Remaining variables were compared across group using independent samples *t*-tests (modified Bonferroni correction). SSRT was calculated for the presession and the ST_{crit} from the presession was set as the most difficult stop time for the scan session. Data are reported as mean ± SE. Significant *P*-values are in bold.

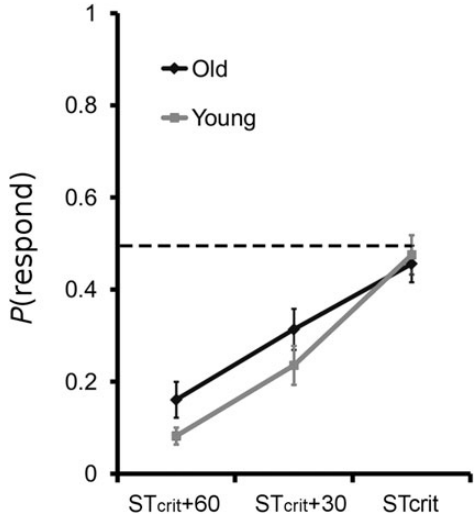

Figure 2. Modulation of stop-task difficulty in the scanner. The closer the stop cue is to the Go response, the greater the probability of responding on a stop trial, confirming our parametric modulation of stop-signal inhibition difficulty during scanning.

of interest using small volume correction. This analysis revealed an interaction within the right IFC (90 voxels; peak MNI: 50, 10, 20; $t = 3.83$; $P = 0.01$) and preSMA (10 voxels; peak MNI: 10, 2, 72; $t = 3.46$; $P = 0.03$; Fig. 3*B*,*C*). The reverse interaction, $(\text{StopInhibit} > \text{Go}_{\text{Old}}) > (\text{StopInhibit} > \text{Go}_{\text{Young}})$, did not reveal any significant results following the procedures outlined above, even after relaxing the height threshold to $P < 0.05$ uncorrected.

Activation Associated with Action Reprogramming

In addition to presenting stop cues, we manipulated whether action reprogramming was additionally required on Stop trials. Therefore, we tested for regions that were more active for Stop one (SL-GR and SR-GL) than Stop both and Go using conjunction analysis in each group.

For the young group, activation was observed in the bilateral supramarginal gyrus, superior partietal lobule (Area 7A), dorsal premotor cortex, SMAproper, and an inferior region of preSMA that is also referred to as the posterior rostral cingulate zone (RCZp; Table 3). Using the same statistical criteria, there were no significant conjunction results for the Old group. This could be interpreted as further evidence of a lack of modulatory capacity in older adults with progressively increasing task difficulty (here referring to Stop one vs. Stop both conditions).

Group Comparisons Between Go and StopInhibit Trials

To determine whether there was any evidence for age-related overactivation or hypoactivation (Grady 2012) for this task, we compared the age groups directly on Go and StopInhibit trials.

The older adults showed increased activation on Go trials in several regions (Old > Young; Fig. 4*A*). The main clusters were in the left (1397 voxels) and right (951 voxels) visual cortex extending from the lingual gyrus (Areas 17 and 18) into area V4, fusiform gyrus, and inferior temporal gyrus (Table 4). In addition, increased activation was observed in SMAproper/paracentral lobule (794 voxels) extending into the superior parietal lobule, and in the dorsolateral prefrontal cortex (DLPFC; 228 voxels). There were no clusters with significantly greater Go trial activation in the young group (i.e., Young > Old).

Older adults demonstrated increased activation on Go trials, but the opposite was seen in some regions for StopInhibit trials (Old < Young; Fig. 4*B*). Older adults showed reduced activation in preSMA (504 voxels) and in the striatum (337 voxels). Reduced striatal activation was observed in the left and right caudate head, and in the right rostral putamen (Table 4). The reverse StopInhibit contrast (Old > Young; Fig. 4*B*) was highly similar to that observed for Go trials.

Microstructural Organization of White Matter Connecting rIFC, preSMA, and STN Is Associated with StopInhibit > Go Activation in Older Adults

We have shown that white matter FA connecting right IFC, preSMA, and STN predicts inhibitory control (SSRT) ability in older adults (Coxon et al. 2012). We therefore used regression analysis to test for a positive association between FA in this structural network and StopInhibit > Go activation in older adults.

A whole-brain analysis with mean FA as a covariate revealed a positive correlation in just one region (Fig. 5). Older adults with higher FA showed stronger activation of preSMA on Stop trials (36 voxels; peak MNI: 10, 15, 58; $t = 4.1$; $P < 0.001$). Comparing groups revealed the positive association between FA and preSMA activation was present for older but not younger adults (42 voxels; peak MNI: 10, 15, 55; $t = 4.53$; $P < 0.001$). The association in the old group was also independent of age (partial correlation $r = 0.48$, $P = 0.039$). Thus, older adults with less deterioration of white matter microstructural organization were better able to recruit preSMA for stop-signal inhibition.

Discussion

We investigated cognitive action control in the form of directed-global inhibition. We sought to determine whether older adults modulate brain activity when engaged in the difficult task of rapidly inhibiting an initiated response. As expected, young adults were faster at stopping and showed activation in right IFC (pars opercularis), preSMA, and the basal ganglia (striatum and STN), regions that together function as a brake on movement (Aron et al. 2014). Older adults did not show significant StopInhibit > Go activation in these regions even though stopping performance was matched. Nor was there evidence of compensatory overactivation during stopping. Instead, older adults had increased activation of visual cortex and DLPFC on Go trials, and hypoactivation of preSMA and striatum (caudate head and rostral putamen) on StopInhibit trials. Within the old group, white matter microstructural organization in a rIFC–preSMA–STN tract mask was positively associated with stopping activation in preSMA. The results suggest that inhibitory control deficits in older adults are associated with less effective recruitment of cortical and subcortical regions, and that maintenance of brain structure may have positive implications for brain function.

Activation During Stop-Signal Inhibition and Action Reprogramming in Young Adults

Stop-signal inhibition is thought to rely on the rapid and global suppression of an initiated motor process, with movement generation interrupted via projections to the basal ganglia (STN

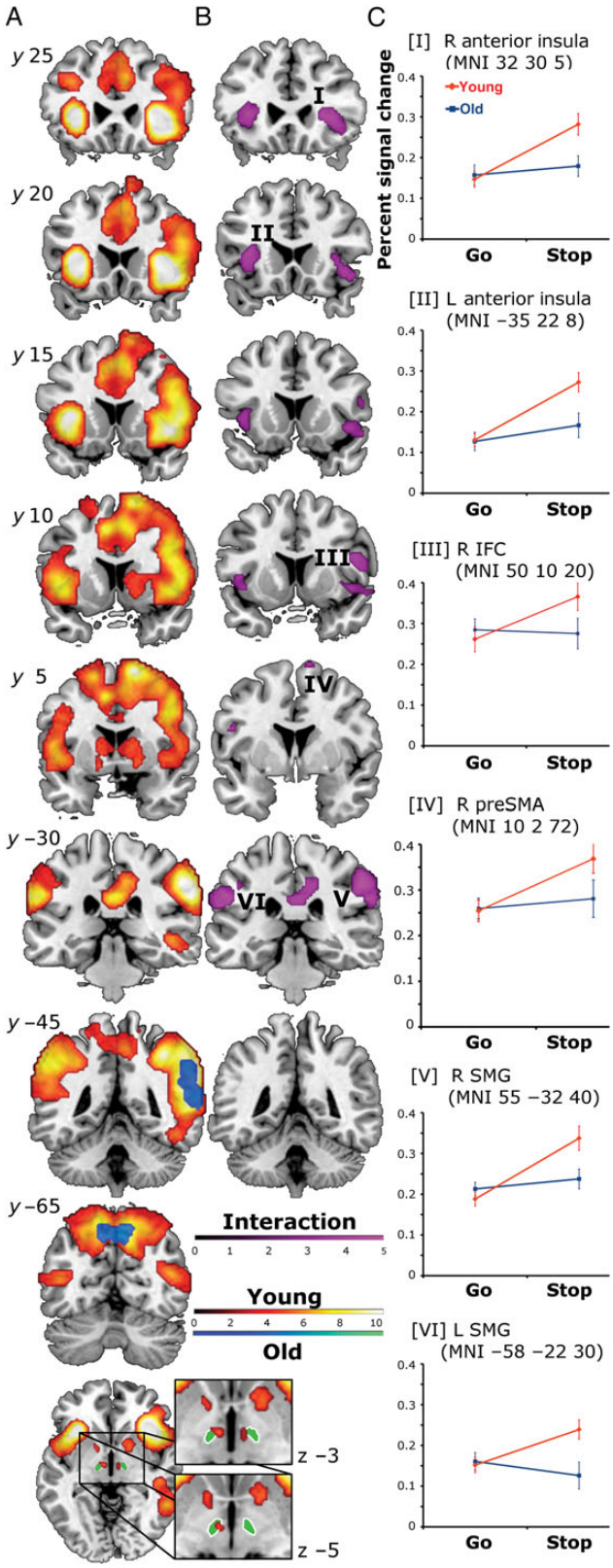

Figure 3. Active regions for the main contrast StopInhibit > Go, corrected for multiple comparisons (FWE $P < 0.05$) at the cluster level. Neurological orientation (right = image right). (*A*) The *t*-values for the young group are shown in the red color scale. Areas previously implicated in response inhibition (right IFC, preSMA, caudate, and STN) are active for the young group only. Structurally delineated STN is shown in green. Activation common to both Young and Old (conjunction, *t*-values shown in blue color scale) was observed in right supramarginal gyrus and SPL (Area 7A). There were no areas of unique activation in the old group. (*B*) The *t*-values for the interaction (StopInhibit > Go_{Young}) > (StopInhibit > Go_{Old}) are shown in the violet color scale. A significant interaction was present in bilateral anterior insula and supramarginal gyrus. The interaction was also significant in right IFC and preSMA at both the voxel and cluster level (FWE $P < 0.05$) after small volume correction. The reverse interaction did not reveal any significant results. (*C*) Percent signal change for Go and StopInhibit in each group at the local maxima shown in *B*. The roman numerals adjacent to the clusters in *B* correspond to the plots in *C*.

and/or striatum) (Coxon et al. 2006; Aron et al. 2007, 2014; Stinear et al. 2009). For our group of young adults, the main contrast of StopInhibit > Go revealed activation within rIFC, preSMA, striatum, and anatomically delineated STN. These regions are consistently implicated in fMRI studies of stop-signal inhibition in young adults (Aron and Poldrack 2006; Zandbelt and Vink 2010; Levy and Wagner 2011; Swick et al. 2011; Zandbelt et al. 2013). Our group of young adults also showed increased activation in ventral preSMA (MNI −2, 2, 48), near the cingulate gyrus on Stop one trials, matching that shown previously (Coxon et al. 2009). This area borders on or overlaps RCZp, known to contribute to complex motor control (Picard and Strick 1996, 2001), and may play a role in action re-programming. The more robust activation compared with our previous work using this task (Coxon et al. 2009) could relate to the larger sample size, stronger field strength, and more difficult stop times.

Activation During Stop-Signal Inhibition in Older Adults

Activation for StopInhibit > Go in the old group was significant in the superior parietal lobe (Area 7a) and right temporoparietal cortex, areas also active in young adults. Area 7a is involved in visual motion processing for interceptive action (Merchant et al. 2004; Merchant and Georgopoulos 2006) and stopping was cued in this domain. The superior parietal lobe is crucial for spatial attention (Yantis et al. 2002) while more ventrally, the right inferior parietal lobe and temporoparietal junction detect behaviorally relevant salient events (Corbetta and Shulman 2002; Husain and Nachev 2007) such as infrequent and temporally uncertain stop cues. Thus, older adults exhibited similar activation to young adults in regions involved in the higher order processing of visual stop cues.

Bilateral supramarginal gyrus, anterior insula, and additionally right IFC and preSMA showed a significant StopInhibit > Go by age interaction. Activation increased for StopInhibit relative to Go for the young but not for the old group. These regions are also implicated in target detection and attention to salient events (Corbetta and Shulman 2002; Eckert et al. 2009; Menon and Uddin 2010). Right IFC and anterior insula are thought to be important for attentional capture (Sharp et al. 2010) and for implementing inhibition (Aron et al. 2003, 2014). The old group clearly detected the occurrence of stop cues and they did show right temporoparietal activation. One potential account of the observed age-related behavioral inhibition deficit is that anterior insula and right IFC did not effectively convey the stop cue to other areas, for example preSMA or STN; however, this requires further investigation.

Previous studies investigating the consequences of aging on inhibition have reported evidence of overactivation in older adults. A common observation has been additional recruitment of left IFC (Nielson et al. 2002; Langenecker and Nielson 2003; Langenecker et al. 2004; Colcombe et al. 2005; Zysset et al.

Table 2
Brain regions active in each group for contrast StopInhibit > Go

Region	Right hemisphere				Left hemisphere			
	MNI (*x*, *y*, *z*)	*t*-value	$Y_{\beta \pm SE}$	$O_{\beta \pm SE}$	MNI (*x*, *y*, *z*)	*t*-value	$Y_{\beta \pm SE}$	$O_{\beta \pm SE}$
Young: cortical—medial								
preSMA	15, 5, 70	10	5.2 ± 0.52	2.6 ± 0.77				
preSMA	8, 12, 50	7.5	3.7 ± 0.50	1.9 ± 0.61	−8, 8, 48	7.9	3.0 ± 0.38	1.9 ± 0.61
PMd	18, −2, 68	8.8	4.0 ± 0.44	2.4 ± 0.76	−18, 0, 67	8.7	4.1 ± 0.46	2.5 ± 0.75
RCZa	8, 28, 32	6.6	2.6 ± 0.39	2.4 ± 0.75	−10, 32, 25	4.2	1.3 ± 0.31	3.0 ± 0.94
SPL (Area 7A)	10, −68, 48	8.8	5.6 ± 0.63	4.2 ± 1.09	−12, −65, 58	8	5.4 ± 0.68	3.8 ± 1.15
Young: cortical—lateral								
IFC: pars opercularis (Area 44)	52, 15, 8	8.9	4.0 ± 0.45	2.5 ± 0.75				
Anterior insula	35, 25, 2	14.3	5.9 ± 0.41	2.5 ± 0.80	−32, 22, 5	13.3	5.5 ± 0.42	2.8 ± 0.85
IFJ	42, 8, 35	7.6	4.2 ± 0.56	2.4 ± 0.74	−45, 5, 25	4.8	2.3 ± 0.48	3.3 ± 1.04
DLPFC	38, 40, 25	7.2	3.3 ± 0.46	2.4 ± 0.76	−38, 32, 32	9	4.1 ± 0.45	3.0 ± 0.94
Supramarginal gyrus	58, −40, 32	12.5	6.6 ± 0.53	3.0 ± 0.91	−55, −38, 35	9.3	4.8 ± 0.52	2.9 ± 0.91
Inferior parietal lobule	38, −48, 50	10	5.6 ± 0.56	3.0 ± 0.89				
Middle temporal gyrus	58, −48, 5	9.1	4.6 ± 0.51	2.9 ± 0.92	−42, −62, 12	5.9	3.0 ± 0.51	2.3 ± 0.73
Young: subcortical								
Caudate nucleus	12, 4, 10	4.7	2.3 ± 0.49	2.4 ± 0.75	−10, 5, 8	4.5	2.6 ± 0.59	2.8 ± 0.85
Pallidum	18, 8, −2	5.1	1.6 ± 0.32	2.4 ± 0.77	−12, 5, −8	3.8	1.3 ± 0.33	2.6 ± 0.82
STN	8, −12, −3	3.3	1.4 ± 0.42	2.5 ± 0.77	−8, −10, −3	3.6	1.4 ± 0.39	2.4 ± 0.77
Thalamus (PFC zone)	8, −10, 5	4.4	2.2 ± 0.50	2.4 ± 0.75				
Old: cortical								
SPL (Area 7A)	5, −65, 48	4.8	4.7 ± 0.67	5.7 ± 1.17	−8, −65, 48	4	3.3 ± 0.56	3.9 ± 0.96
Inferior parietal lobule	58, −48, 38	3.8	4.6 ± 0.53	3.5 ± 0.91				
Middle temporal gyrus	62, −48, 18	4.5	4.3 ± 0.52	4.1 ± 0.91				

Note: MNI coordinates and *t*-values are specific to either the young or the old group and reflect local maxima within the cluster (22 128 voxels). Parameter estimates (β) and standard errors (SE) are shown for qualitative comparison of model fit in each group.
preSMA, presupplementary motor area; RCZa, anterior rostral cingulate zone; PMd, dorsal premotor cortex; SPL, superior parietal lobe; IFC, inferior frontal cortex; IFJ, inferior frontal junction; DLPFC, dorsolateral prefrontal cortex; STN, subthalamic nucleus.

Table 3
Brain regions associated with action reprogramming on Stop one trials

Region	Right hemisphere				Left hemisphere			
	MNI (*x*, *y*, *z*)	*t*-value	$Y_{\beta \pm SE}$	$O_{\beta \pm SE}$	MNI (*x*, *y*, *z*)	*t*-value	$Y_{\beta \pm SE}$	$O_{\beta \pm SE}$
Young: cortical—medial								
preSMA/RCZp	8, 10, 42	4.0	7.7 ± 0.57	4.8 ± 0.66	−2, 2, 48	4.7	11.6 ± 0.78	6.9 ± 0.91
SMAproper	15, −2, 75	5.3	10.2 ± 0.87	7.5 ± 1.0				
PMd	28, −2, 65	4.9	10.4 ± 0.81	8.2 ± 0.93	−20, −5, 72	4.2	10.2 ± 0.80	6.8 ± 0.93
PMd/FEF	30, −8, 55	4.8	6.5 ± 0.50	5.2 ± 0.58	−30, −8, 55	4.7	7.55 ± 0.61	4.9 ± 0.71
SPL (Area 7a)	18, −52, 65	5.2	7.3 ± 0.65	3.6 ± 0.76	−15, −55, 65	5.4	7.9 ± 0.66	6.1 ± 0.77
Young: cortical—lateral								
Supramarginal gyrus	58, −25, 40	6.1	10.0 ± 0.61	5.7 ± 0.71	−58, −22, 30	5.9	6.2 ± 0.48	3.4 ± 0.56
Inferior parietal lobule	38,−38, 48	5.2	8.6 ± 0.63	6.7 ± 0.73				

Note: Active regions for the conjunction SL-GR > SA ∩ SL-GR > Go ∩ SR-GL > SA ∩ SR-GL > Go, corrected for multiple comparisons (FWE $P < 0.05$) at the cluster level.
MNI coordinates and *t*-values are specific to the young group. No significant clusters were observed in the old group. Parameter estimates (β) and standard errors (SE) are shown for qualitative comparison of model fit in each group.
preSMA, presupplementary motor area; RCZp, posterior rostral cingulate zone; SMAproper, supplementary motor area; PMd, dorsal premotor cortex; FEF, frontal eye fields; SPL, superior parietal lobe.

2007; Vallesi et al. 2011), but there is also evidence to suggest enhanced activity of the same regions seen in young adults (Turner and Spreng 2012). Vallesi et al. (2011) showed overactivation in frontoparietal regions for a Stroop-like Go/Nogo decision task. They manipulated task demands by increasing the complexity of the stimulus-response mapping as opposed to placing time constraints on inhibitory control and accuracy was around 90% for the most difficult condition. It seems that older adults may be able to compensate by recruiting more neural resources (Reuter-Lorenz and Cappell 2008; Grady 2012) when faced with the requirement to filter out distracting information (indirect-competitive inhibition), forgoing speed to maintain acceptable accuracy on the task. It may therefore be somewhat surprising that we did not find evidence of age-related overactivation during inhibition in the present study. However, the aforementioned studies primarily dealt with the effects of aging on the indirect-competitive form of inhibition and overall accuracy was relatively high. In contrast, our paradigm targeted directed-global inhibition and stop trial accuracy approached 50%.

By investigating inhibitory control near the critical stop latency, probing a directed-global form of inhibition, we found a relative lack of modulation on StopInhibit trials in our group of older adults. This finding is consistent with the compensation-related utilization of neural circuits hypothesis, which predicts that older adults plateau at a level where young adults are still able to increase brain activity (Reuter-Lorenz and Cappell 2008; Grady 2012). It also complements a recent lifespan stop-signal study, reporting that right IFC activation decreases with age across the adult lifespan (Sebastian et al. 2013). We also show that modulation of activation in secondary motor areas on Stop one trials is absent in older adults. The

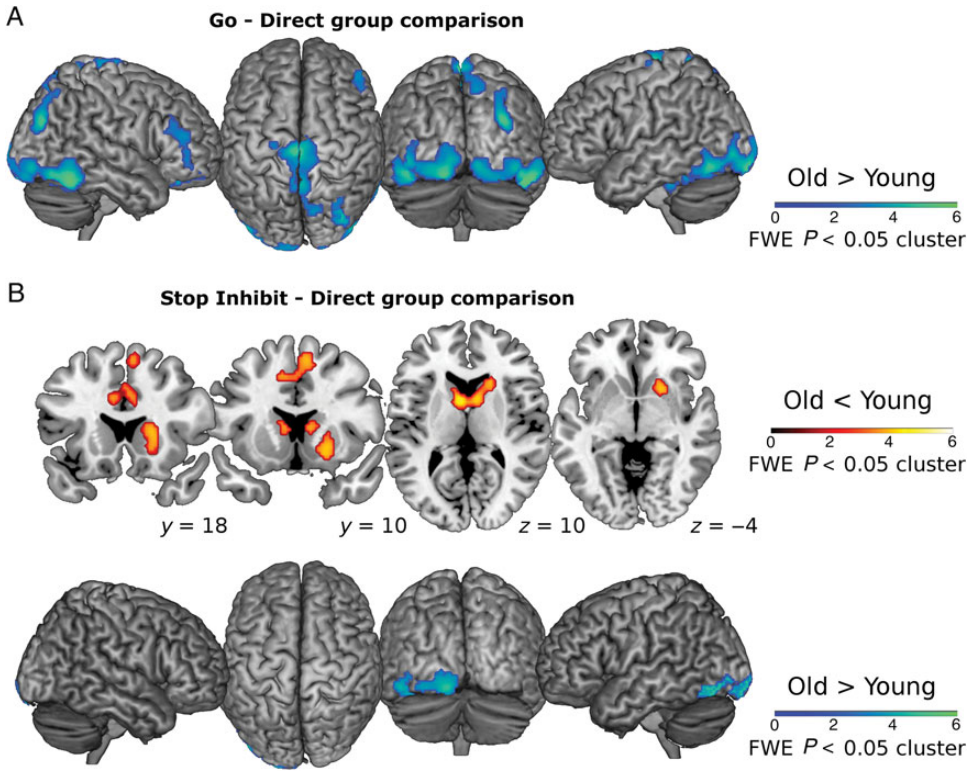

Figure 4. Direct group comparison of activation on Go trials (*A*) and StopInhibit trials (*B*). Results are corrected for multiple comparisons (FWE $P < 0.05$) at the cluster level.

Table 4
Brain regions for direct contrasts of group activation

Region	Right hemisphere				Left hemisphere			
	MNI (*x*, *y*, *z*)	*t*-value	$Y_{\beta \pm SE}$	$O_{\beta \pm SE}$	MNI (*x*, *y*, *z*)	*t*-value	$Y_{\beta \pm SE}$	$O_{\beta \pm SE}$
Go: Old > Young								
Lingual gyrus (Area 17)	12, −92, −8	4.5	1.1 ± 0.33	3.5 ± 0.42	−15, −98, −15	4.5	1.2 ± 0.37	4.3 ± 0.51
Lingual gyrus (Area 18)	15, −90, −10	4.5	1.3 ± 0.33	3.6 ± 0.44	−10, −98, −2	5.6	1.1 ± 0.32	3.7 ± 0.45
Fusiform gyrus	35, −58, −18	3.8	2.4 ± 0.27	4.0 ± 0.34	−40, −58, −15	5.5	1.1 ± 0.19	2.8 ± 0.24
V4	42, −85, −10	4.6	2.4 ± 0.30	4.6 ± 0.38	−32, −72, −15	3.7	2.3 ± 0.28	4.0 ± 0.36
Inferior temporal gyrus	50, −55, −20	5.8	1.3 ± 0.27	3.9 ± 0.34				
SMAproper					−2, −22, 72	5.3	1.1 ± 0.31	3.1 ± 0.42
SPL: Precuneus	10, −72, 55	3.8	2.7 ± 0.47	5.6 ± 0.59				
Middle occipital gyrus	32, −75, 30	5.6	2.2 ± 0.28	4.7 ± 0.35				
DLPFC	48, 40, 18	3.8	0.75 ± 0.24	2.2 ± 0.31				
StopInhibit: Old < Young								
preSMA	8, 10, 55	4.0	9.3 ± 0.80	4.6 ± 0.86	−10, 8, 45	3.9	7.8 ± 0.54	4.7 ± 0.59
RCZa	5, 28, 25	3.8	4.3 ± 0.71	1.9 ± 0.53	−8, 20, 30	3.9	4.8 ± 0.60	2.0 ± 0.57
Caudate nucleus	8, 8, 10	4.3	6.4 ± 0.95	3.0 ± 0.86	−5, 5, 10	4.7	6.9 ± 1.04	3.1 ± 0.92
Putamen	20, 12, −10	4.0	5.9 ± 0.62	2.2 ± 0.67				

Note: MNI coordinates and *t*-values are specific to the group comparison. Parameter estimates (β) and standard errors (SE) are shown for qualitative comparison of model fit in each group. SMAproper, supplementary motor area; preSMA, presupplementary motor area; RCZa, anterior rostral cingulate zone; DLPFC, dorsolateral prefrontal cortex.

overall picture is that response inhibition and action reprogramming, when performed under high difficulty levels (i.e., 50% success), are not associated with increased Stop versus Go recruitment or overactivation in older adults. Despite using an ANOVA model that assumed unequal variance between groups, increased interindividual variability among older adults may have contributed to this result. However, it is clear from the plots in Figure 3, and the parameter estimates (Tables 2–4) that there was activation above baseline in the old group. fMRI only allows for relative differences between conditions and groups. It is likely that older adults did use the same or similar circuitry for response inhibition as young adults, except there was less differentiation between the Stop and Go conditions.

When group activation was compared for Go and StopInhibit trials separately, increased activation was observed for older adults in the occipital and parietal lobes. Older adults may utilize a more global attention network than young adults to meet the requirements of our task. Older adults also had increased right DLPFC activation on Go trials. Right DLPFC overactivation has been observed in previous bimanual coordination studies of aging (Coxon et al. 2010; Goble et al. 2010). It has been argued that DLPFC implements task rules maintained in

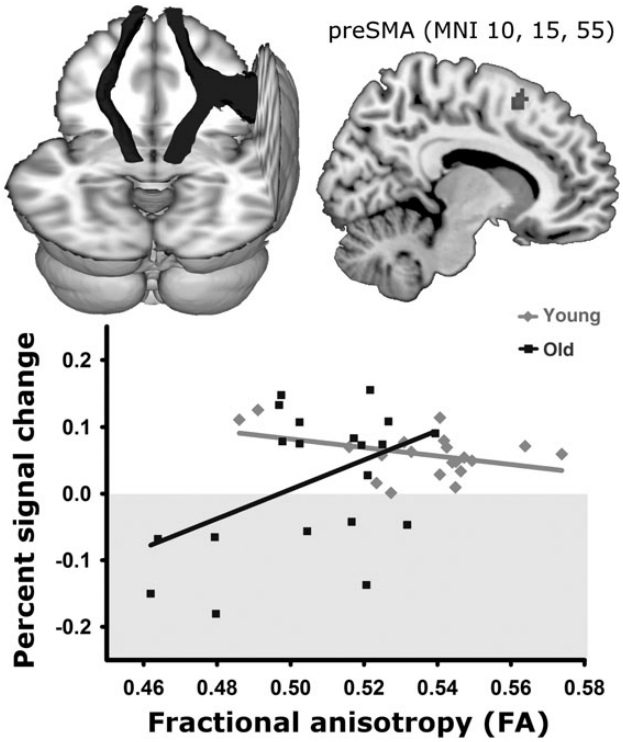

Figure 5. StopInhibit > Go activation regressed against mean FA from a combined rIFC–preSMA–STN tract mask (top left). Older adults with less white matter deterioration were better able to activate preSMA (top right), and this same cluster remained for the group comparison. Percent signal change is plotted against FA below. Negative percent signal change (light gray shaded region) indicates that, for some old participants, activation was greater for Go than StopInhibit.

working memory rather than inhibition (Aron et al. 2014), and it is possible that the increased DLPFC activity reflects a heightened anticipation of the requirement to stop on trials that turn out to be Go trials. In contrast to Go trials, the group comparison for StopInhibit revealed hypoactivation of preSMA and anterior regions of the striatum (caudate head and rostral putamen) in older adults. These same regions were more active for StopInhibit than Go in young adults in our study (compare Figs 3*A* and 5*B*), and in previous research (for meta-analysis, see Swick et al. 2011). Anterior regions of the striatum have been implicated in both the implementation of inhibition and in setting up an inhibitory response set to improve stopping performance (Vink et al. 2005; Zandbelt and Vink 2010; Majid et al. 2013). Taken together, the pattern of group differences suggests more effortful attention to the task in older adults, perhaps in an attempt to counteract less effective implementation of inhibition by regions such as the preSMA and basal ganglia. Whether stopping deficits in older adults relate specifically to proactive inhibition is a potential avenue for future research.

Functional Modulation and Behavior in Older Adults Are Associated with Microstructural Organization of White Matter Connecting rIFC, preSMA, and STN

Interindividual variability of white matter tracts connecting right IFC, preSMA, and STN predicts inhibitory control (SSRT) ability in older adults (Coxon et al. 2012). Therefore, we tested the hypothesis that StopInhibit > Go activation is associated with white matter microstructural organization in these tracts in older adults. Consistent with the notion that brain structure constrains function, and in turn determines behavior, older adults with higher FA were better able to activate preSMA, one of the key cortical regions implicated in inhibitory control. While it is tempting to conclude that less white matter deterioration or better maintained microstructural organization has positive implications for brain function, we acknowledge that there are many mechanisms by which the diffusion-weighted signal can be modulated (Jones et al. 2013). Our results complement previous studies showing associations between behavior, task-related functional modulation, and either white matter density (Colcombe et al. 2005) or hyperintensity volume (Hedden et al. 2012). Our approach differed in that we extracted information from task-specific tracts. It is possible that individual differences in genetics and lifestyle factors account for the observed variation in older adults' structural network integrity, functional modulation, and behavioral performance (Grady 2012; Nyberg et al. 2012).

In summary, the young group showed a pattern of brain activity typical for directed-global inhibition with activation of rIFC, preSMA, and basal ganglia nuclei. For older adults, we found no evidence of overactivation during response inhibition. Instead, older adults showed a relative lack of modulation for stopping versus going, and reduced activation in preSMA and anterior striatum on Stop trials. Notably, increased white matter integrity in a structural network connecting rIFC, preSMA, and STN was associated with stronger preSMA activation in older adults. The results suggest that inhibitory control deficits are associated with less effective recruitment of task-specific cortical and subcortical regions in some older adults, and that maintenance of brain structure may have positive implications for brain function.

Funding

This work was supported by grants from the Research Fund of the KU Leuven, Belgium (OT/11/071), the Flanders Fund for Scientific Research (G0721.12 and G0708.14), and Grant P7/11 from the Inter-University Attraction Poles Program of the Belgian Federal Government. J.C. was supported by the Flanders Fund for Scientific Research (1224010N) and the Aotearoa Foundation.

Notes

Conflict of Interest: None declared.

References

Aron AR. 2007. The neural basis of inhibition in cognitive control. Neuroscientist. 13:214–228.

Aron AR, Durston S, Eagle DM, Logan GD, Stinear CM, Stuphorn V. 2007. Converging evidence for a fronto-basal-ganglia network for inhibitory control of action and cognition. J Neurosci. 27: 11860–11864.

Aron AR, Fletcher PC, Bullmore ET, Sahakian BJ, Robbins TW. 2003. Stop-signal inhibition disrupted by damage to right inferior frontal gyrus in humans. Nat Neurosci. 6:115–116.

Aron AR, Poldrack RA. 2006. Cortical and subcortical contributions to Stop signal response inhibition: role of the subthalamic nucleus. J Neurosci. 26:2424–2433.

Aron AR, Robbins TW, Poldrack RA. 2014. Inhibition and the right inferior frontal cortex: one decade on. Trends Cogn Sci. 18:177–185.

Bedard AC, Nichols S, Barbosa JA, Schachar R, Logan GD, Tannock R. 2002. The development of selective inhibitory control across the life span. Dev Neuropsychol. 21:93–111.
Behrens TE, Berg HJ, Jbabdi S, Rushworth MF, Woolrich MW. 2007. Probabilistic diffusion tractography with multiple fibre orientations: what can we gain? Neuroimage. 34:144–155.
Bissett PG, Logan GD. 2014. Selective stopping? Maybe not. J Exp Psychol Gen. 143:455–472.
Cabeza R. 2002. Hemispheric asymmetry reduction in older adults: the HAROLD model. Psychol Aging. 17:85–100.
Cabeza R, Anderson ND, Locantore JK, McIntosh AR. 2002. Aging gracefully: compensatory brain activity in high-performing older adults. Neuroimage. 17:1394–1402.
Clapp WC, Rubens MT, Sabharwal J, Gazzaley A. 2011. Deficit in switching between functional brain networks underlies the impact of multitasking on working memory in older adults. Proc Natl Acad Sci USA. 108:7212–7217.
Colcombe SJ, Kramer AF, Erickson KI, Scalf P. 2005. The implications of cortical recruitment and brain morphology for individual differences in inhibitory function in aging humans. Psychol Aging. 20:363–375.
Corbetta M, Shulman GL. 2002. Control of goal-directed and stimulus-driven attention in the brain. Nat Rev Neurosci. 3:201–215.
Coxon JP, Goble DJ, Van Impe A, De Vos J, Wenderoth N, Swinnen SP. 2010. Reduced basal ganglia function when elderly switch between coordinated movement patterns. Cereb Cortex. 20:2368–2379.
Coxon JP, Stinear CM, Byblow WD. 2006. Intracortical inhibition during volitional inhibition of prepared action. J Neurophysiol. 95:3371–3383.
Coxon JP, Stinear CM, Byblow WD. 2007. Selective inhibition of movement. J Neurophysiol. 97:2480–2489.
Coxon JP, Stinear CM, Byblow WD. 2009. Stop and go: the neural basis of selective movement prevention. J Cogn Neurosci. 21:1193–1203.
Coxon JP, Van Impe A, Wenderoth N, Swinnen SP. 2012. Aging and inhibitory control of action: cortico-subthalamic connection strength predicts stopping performance. J Neurosci. 32:8401–8412.
Eckert MA, Menon V, Walczak A, Ahlstrom J, Denslow S, Horwitz A, Dubno JR. 2009. At the heart of the ventral attention system: the right anterior insula. Hum Brain Mapp. 30:2530–2541.
Gazzaley A, Cooney JW, McEvoy K, Knight RT, D'Esposito M. 2005. Top-down enhancement and suppression of the magnitude and speed of neural activity. J Cogn Neurosci. 17:507–517.
Goble DJ, Coxon JP, Van Impe A, De Vos J, Wenderoth N, Swinnen SP. 2010. The neural control of bimanual movements in the elderly: brain regions exhibiting age-related increases in activity, frequency-induced neural modulation, and task-specific compensatory recruitment. Hum Brain Mapp. 31:1281–1295.
Grady C. 2012. The cognitive neuroscience of ageing. Nat Rev Neurosci. 13:491–505.
Hasher L, Zacks RT. 1988. Working memory, comprehension, and aging: a review and a new view. In: Bower GH, editor. The psychology of learning and motivation. New York, NY: Academic Press. p. 193–225.
Healey MK, Campbell KL, Hasher L. 2008. Cognitive aging and increased distractibility: costs and potential benefits. Prog Brain Res. 169:353–363.
Hedden T, Van Dijk KR, Shire EH, Sperling RA, Johnson KA, Buckner RL. 2012. Failure to modulate attentional control in advanced aging linked to white matter pathology. Cereb Cortex. 22:1038–1051.
Husain M, Nachev P. 2007. Space and the parietal cortex. Trends Cogn Sci. 11:30–36.
Jones DK, Knosche TR, Turner R. 2013. White matter integrity, fiber count, and other fallacies: the do's and don'ts of diffusion MRI. Neuroimage. 73:239–254.
Kelso JA, Southard DL, Goodman D. 1979. On the nature of human interlimb coordination. Science. 203:1029–1031.
Kramer AF, Humphrey DG, Larish JF, Logan GD, Strayer DL. 1994. Aging and inhibition: beyond a unitary view of inhibitory processing in attention. Psychol Aging. 9:491–512.
Langenecker SA, Nielson KA. 2003. Frontal recruitment during response inhibition in older adults replicated with fMRI. Neuroimage. 20:1384–1392.
Langenecker SA, Nielson KA, Rao SM. 2004. fMRI of healthy older adults during Stroop interference. Neuroimage. 21:192–200.
Levy BJ, Wagner AD. 2011. Cognitive control and right ventrolateral prefrontal cortex: reflexive reorienting, motor inhibition, and action updating. Ann N Y Acad Sci. 1224:40–62.
Lustig C, Hasher L, Zacks RT. 2007. Inhibitory deficit theory: recent developments in a 'new view'. In: Gorfein DS, MacLeod CM, editors. The place of inhibition in cognition. Washington, DC: American Psychological Association. p. 145–162.
Macdonald HJ, Stinear CM, Byblow WD. 2012. Uncoupling response inhibition. J Neurophysiol. 108:1492–1500.
Majid DS, Cai W, Corey-Bloom J, Aron AR. 2013. Proactive selective response suppression is implemented via the basal ganglia. J Neurosci. 33:13259–13269.
Menon V, Uddin LQ. 2010. Saliency, switching, attention and control: a network model of insula function. Brain Struct Funct. 214:655–667.
Merchant H, Battaglia-Mayer A, Georgopoulos AP. 2004. Neural responses in motor cortex and area 7a to real and apparent motion. Exp Brain Res. 154:291–307.
Merchant H, Georgopoulos AP. 2006. Neurophysiology of perceptual and motor aspects of interception. J Neurophysiol. 95:1–13.
Munakata Y, Herd SA, Chatham CH, Depue BE, Banich MT, O'Reilly RC. 2011. A unified framework for inhibitory control. Trends Cogn Sci. 15:453–459.
Nichols T, Brett M, Andersson J, Wager T, Poline JB. 2005. Valid conjunction inference with the minimum statistic. Neuroimage. 25:653–660.
Nielson KA, Langenecker SA, Garavan H. 2002. Differences in the functional neuroanatomy of inhibitory control across the adult life span. Psychol Aging. 17:56–71.
Nyberg L, Lovden M, Riklund K, Lindenberger U, Backman L. 2012. Memory aging and brain maintenance. Trends Cogn Sci. 16:292–305.
Picard N, Strick PL. 2001. Imaging the premotor areas. Curr Opin Neurobiol. 11:663–672.
Picard N, Strick PL. 1996. Motor areas of the medial wall: a review of their location and functional activation. Cereb Cortex. 6:342–353.
Reuter-Lorenz PA, Cappell KA. 2008. Neurocognitive aging and the compensation hypothesis. Curr Dir Psychol Sci. 17:177–182.
Sebastian A, Baldermann C, Feige B, Katzev M, Scheller E, Hellwig B, Lieb K, Weiller C, Tuscher O, Kloppel S. 2013. Differential effects of age on subcomponents of response inhibition. Neurobiol Aging. 34:2183–2193.
Sharp DJ, Bonnelle V, De Boissezon X, Beckmann CF, James SG, Patel MC, Mehta MA. 2010. Distinct frontal systems for response inhibition, attentional capture, and error processing. Proc Natl Acad Sci USA. 107:6106–6111.
Stinear CM, Coxon JP, Byblow WD. 2009. Primary motor cortex and movement prevention: where Stop meets Go. Neurosci Biobehav Rev. 33:662–673.
Swick D, Ashley V, Turken U. 2011. Are the neural correlates of stopping and not going identical? Quantitative meta-analysis of two response inhibition tasks. Neuroimage. 56:1655–1665.
Swinnen SP. 2002. Intermanual coordination: from behavioural principles to neural-network interactions. Nat Rev Neurosci. 3:348–359.
Swinnen SP, Wenderoth N. 2004. Two hands, one brain: cognitive neuroscience of bimanual skill. Trends Cogn Sci. 8:18–25.
Tanji J, Okano K, Sato KC. 1988. Neuronal activity in cortical motor areas related to ipsilateral, contralateral, and bilateral digit movements of the monkey. J Neurophysiol. 60:325–343.
Turner GR, Spreng RN. 2012. Executive functions and neurocognitive aging: dissociable patterns of brain activity. Neurobiol Aging. 33:826.e1–826.e13.
Vallesi A, McIntosh AR, Stuss DT. 2011. Overrecruitment in the aging brain as a function of task demands: evidence for a compensatory view. J Cogn Neurosci. 23:801–815.

Vink M, Kahn RS, Raemaekers M, van den Heuvel M, Boersma M, Ramsey NF. 2005. Function of striatum beyond inhibition and execution of motor responses. Hum Brain Mapp. 25:336–344.
Wenderoth N, Van Dooren M, Vandebroek A, De Vos J, Vangheluwe S, Stinear CM, Byblow WD, Swinnen SP. 2009. Conceptual binding: integrated visual cues reduce processing costs in bimanual movements. J Neurophysiol. 102:302–311.
Wessel JR, Aron AR. 2013. Unexpected events induce motor slowing via a brain mechanism for action-stopping with global suppressive effects. J Neurosci. 33:18481–18491.
Williams BR, Ponesse JS, Schachar RJ, Logan GD, Tannock R. 1999. Development of inhibitory control across the life span. Dev Psychol. 35:205–213.
Yantis S, Schwarzbach J, Serences JT, Carlson RL, Steinmetz MA, Pekar JJ, Courtney SM. 2002. Transient neural activity in human parietal cortex during spatial attention shifts. Nat Neurosci. 5:995–1002.
Zandbelt BB, Bloemendaal M, Hoogendam JM, Kahn RS, Vink M. 2013. Transcranial magnetic stimulation and functional MRI reveal cortical and subcortical interactions during stop-signal response inhibition. J Cogn Neurosci. 25:157–174.
Zandbelt BB, Vink M. 2010. On the role of the striatum in response inhibition. PLoS ONE. 5:e13848.
Zysset S, Schroeter ML, Neumann J, von Cramon DY. 2007. Stroop interference, hemodynamic response and aging: an event-related fMRI study. Neurobiol Aging. 28:937–946.